Journal of Immunological Methods 471 (2019) 18–26

Contents lists available at ScienceDirect

Journal of Immunological Methods

journal homepage: www.elsevier.com/locate/jim

Highly sensitive chemiluminescence enzyme immunoassay for the quantification of carcinoembryonic antigen in the presence of an enhancer and a stabilizer

Seung Sun Kim[a,b], Yujung Lee[a], Hyung Shik Shin[b,*], Ji Hoon Lee[a,*]

[a] Luminescent MD, LLC, Hagerstown, MD 20877, United States
[b] School of Chemical Engineering, Chonbuk University, Jeonju, Jeonbuk 54896, Republic of Korea

ARTICLE INFO

Keywords:
Chemiluminescence enzyme immunoassay (CLEIA)
Enhancer
1,1′-oxalyldiimidazole chemiluminescence (ODI-CL)
Phenol red derivatives
Carcinoembryonic antigen (CEA)
Horseradish peroxidase (HRP)

ABSTRACT

Using the advantages of phenol red, a signal enhancer, and bovine serum albumin (BSA), a stabilizer of horseradish peroxidase (HRP), added in HRP enzyme reaction of Amplex Red and H_2O_2, highly sensitive 1,1′-oxalyldiimidazole chemiluminescence enzyme immunoassay (ODI-CLEIA) was developed to rapidly quantify trace levels of carcinoembryonic antigen (CEA) in human serum. Phenol red acts as an enhancer in ODI-CLEIA while BSA supported rapid and stable activation of HRP. The CL emission of resorufin formed from the HRP enzyme reaction in the presence of BSA and phenol red was about 70-fold brighter than that in the absence of both materials. ODI-CLEIA in the presence of BSA (1.5 mg/ml).and phenol red (1 mM) was able to rapidly analyze CEA in human serum with the wide linear calibration curve (2.5–100 ng/ml). The limit of detection (LOD = 3σ/slope) of ODI-CLEIA was as low as 0.19 ng/ml. Additionally, it was confirmed that the accuracy, precision, and reproducibility of ODI-CLEIA in the presence of BSA and phenol red were good with the statistically acceptable error range.

1. Introduction

Enzyme linked immunosorbent assay (ELISA) using a rabbit antibody conjugated with alkaline phosphatase (ALP) was reported for the first time in 1971 (Engvall and Perlmann, 1971) to solve the major concerns (e.g., the health issue of laboratory personnel, the treatment of radioactive wastes) of radioimmunoassay (RIA) operated with an antibody conjugated with iodine-125. Unfortunately, the sensitivity of ELISA wasn't as good as that of RIA (Engvall and Perlmann, 1971). In order to solve the disadvantages of the conventional ELISA, more advanced enzyme immunoassays (EIAs) have been developed (Rongen et al., 1994; Pei et al., 2013; Chen et al., 2017; Sakamoto et al., 2018). For example, relatively cost-effective horseradish peroxidase (HRP), instead of ALP, has been applied as a powerful enzyme in EIAs with various optical sensors such as chemiluminescence (Vdovenko et al., 2010; Bodulev et al., 2018), colorimetric (Liu et al., 2010; Vashist et al., 2015), and fluorescence (Ahn et al., 2015; Wu et al., 2018). EIAs with a luminol (Yang et al., 2010; Feng et al., 2014) or 1,1′-oxalyldiimidazole (ODI) (Chong et al., 2013; Choi et al., 2017) chemiluminescence detection were more sensitive than EIAs with the rest optical detections. The sensitivity of chemiluminescence EIAs (CLEIAs) operated with HRP has been improved with the addition of an enhancer such as 3(10′-phenothiazinyl)propionic acid/N-morpholinopyridine pair (Yu et al., 2011; Vdovenko et al., 2012), 4-(1,2,4-triazol-1-yl) phenol (Liu et al., 2015), 4-(1-imidazolyl) phenol (Dotsikas and Loukas, 2004; Yusakul et al., 2015), bromophenl red (Yu et al., 2016), and *p*-iodophenol (Kim et al., 2014; Liu et al., 2016).

As shown in Scheme 1, ODI-CL enzyme assay in the presence of HRP needs a non-luminescent substrate, Amplex Red, **4**, capable of transferring to luminescent probe, resorufin, **5**, from the enzyme reaction between Amplex read and H_2O_2 in the presence of HRP (Choi et al., 2010; Lee et al., 2010; Park et al., 2011; Lee et al., 2019). This is because the high-energy intermediate, **X**, formed from the reaction of ODI and H_2O_2 acts as a donor like a light source (e.g., Xenon lamp, laser) used to generate fluorescence (Lee et al., 2002; Park et al., 2011; Park et al., 2013). In order to emit bright light in ODI-CL enzyme reaction, first, resorufin formed from HRP enzyme reaction is activated by the high-energy intermediate based on the principle of chemically induced electron exchange luminescence (CIEEL) process (Lee et al., 2002). Then, resorufin under the excited state emit bright red light. Thus, an enhancer used to improve the sensitivity of ODI CLEIA should be added in the enzyme reaction of Amplex Red and H_2O_2 in the presence of HRP

---

* Corresponding authors.
E-mail addresses: hsshin@jbnu.ac.kr (H.S. Shin), jhlee@luminescentmd.com (J.H. Lee).

https://doi.org/10.1016/j.jim.2019.05.003
Received 6 March 2019; Received in revised form 26 April 2019; Accepted 22 May 2019

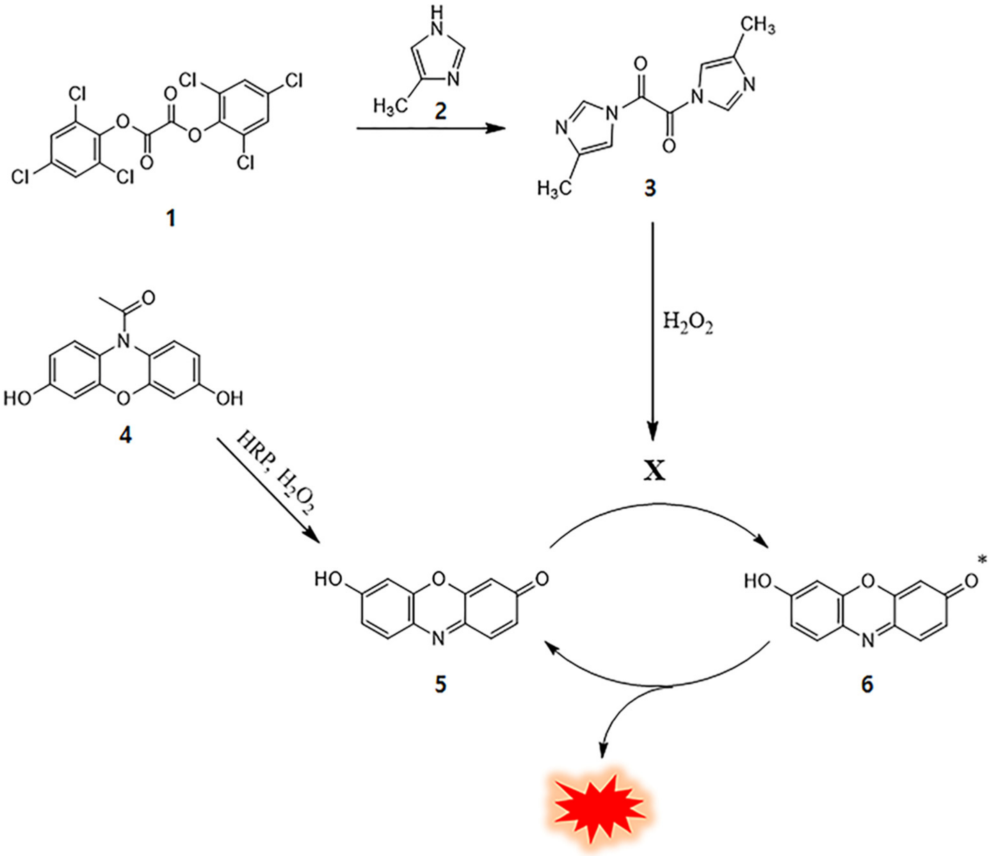

Scheme 1. Enzyme (HRP) assay with ODI-CL detection. **1**. TCPO, **2**. 4-methylimidazole, **3**. ODI, **4**. Amplex Red, **5**. resorufin under the ground state, **6**. Resorufin under the excited state, **X**. high-energy intermediate.

to rapidly produce the high concentration of resorufin before the ODI-CL reaction.

Scheme 1 indicates that the procedure of ODI CLEIA is completely different from that of luminol CLEIA. This is because ODI has been used as a reagent to produce the high-energy intermediate capable of transferring energy to resorufin, whereas luminol (Barni et al., 2007) acts directly as a substrate like Amplex Red in ODI CLEIA. Due to the apparent differences of the both CLEIAs, for example, the efficiency of *p*-iodophenol applied as an enhancer in ODI-CLEIAs (Kim et al., 2014) was different from that in luminol CLEIA (Liu et al., 2016).

Recently, Yu and his/her collaborators reported that bromophenol red, widely applied as a chemical indicator, can be used a strong enhancer in luminol enzyme assay for the quantification of a specific DNA (Yu et al., 2016). The report indicates that various chemical indicators, such as phenol red, chlorophenol red, bromophenol red, and bromophenol blue, can be a candidate capable of improving the sensitivity of ODI CLEIA. Based on the hypothesis, we studied the roles of phenol derivatives in ODI CLEIA for the quantification of carcinoembryonic antigen (CEA), known as one of the tumor markers. Details are described as shown below.

2. Experimental

2.1. Chemicals and materials

Carcinoembryonic antigen (CEA), alpha-fetoprotein (AFP), and prostate specific antigen (PSA) were purchased from Lee Biosolutions. Vascular Endothelial Growth Factor (VEGF), Cancer Antigen 19–9 (CA 19–9), and Glypican 1 (GPC-1) were purchased from Thermo Scientific. CEA ELISA kit and a diluent (0 calibrator matrix) were purchased from Monobind. Horseradish peroxidase, phenol red, bromophenol red, bromophenol blue, chlorophenol red, bovine serum albumin (BSA), and resorufin were purchased from MilliporeSigma. Amplex Red was purchased from Cayman Chemical. Isopropyl alcohol (HPLC grade), ethyl acetate (HPLC grade), ultrapure deionized water, and H_2O_2 (30%) were purchased from VWR. Human serum samples collected from patients were provided by Meritus Medical Center located in Hagerstown, MD, Untied States.

2.2. Effect of phenol derivatives in HRP enzyme assay with ODI-CL detection

In order to study the roles of phenol derivatives, 1 μM Amplex Red (60 μl) was added in a 1.5-ml microcentrifuge tube containing the mixture (60 μl) of HRP (2 mU/ml) and 1.5 mM H_2O_2 in the absence and presence of phenol red, bromophenol red, bromophenol blue, or chlorophenol red (1 mM). Resorufin was formed in the centrifuge tube while the final mixture was incubated at room temperature (21 ± 3 °C). Resorufin (20 μl) formed in each microcentrifuge tube after the incubation for a certain time was transferred into a borosilicated test tube. The test tube was inserted immediately to the detection cell of a luminometer with two syringe pumps (Lumat 9507, Berthold). Then, relative CL intensity of light emitted in the test tube was measured for 2 s after injecting H_2O_2 (25 μl) and ODI (25 μl) into the test tube using the two syringe pumps. Using the experimental data measured under different conditions, the effect of phenol derivatives in HRP enzyme assay was studied.

2.3. Effect of BSA in HRP enzyme assay in the presence of phenol red in sodium phosphate buffer (pH 8)

6 different concentrations of BSA from 0 to 4 mg/ml in 20 mM

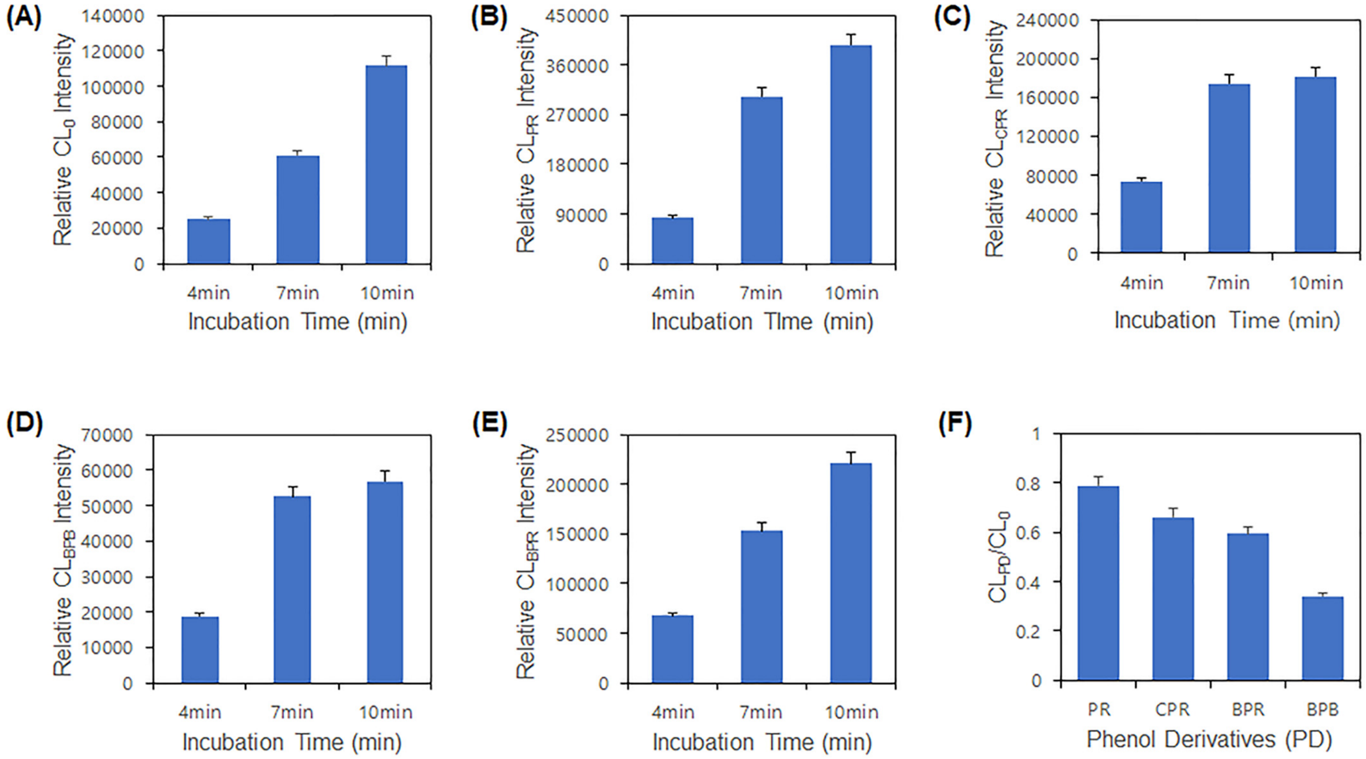

Fig. 1. (A) ODI-CL enzyme reaction in the absence of phenol derivatives (PD), (B) ODI-CL enzyme reaction in the presence of PR, (C) ODI-CL enzyme reaction in the presence of CPR, (D) ODI-CL enzyme reaction in the presence of BPB, (E) ODI-CL enzyme reaction in the presence of BPR, (F) Quenching effect of PD in ODI-CL reaction in the presence of resorufin. Reaction condition: (A~E) [HRP] = 1 mU/ml, [Amplex Red] = 1 μM, [H_2O_2] = 1.0 mM, and [PD] = 1 mM in 10 mM Tris–HCl (pH 8). (F) [Resorufin] = 10 μM and [PD] = 1 mM in 10 mM Tris–HCl (pH 8). (For interpretation of the references to colour in this figure legend, the reader is referred to the web version of this article.)

sodium phosphate buffer (pH 8). Each BSA solution (20 μl) was mixed with 20 mM sodium phosphate buffer (40 μl) contacting HRP (2 mU/ml), H_2O_2 (1.5 mM) and phenol red (1 mM). Then, 1 μM Amplex Red (60 μl) in 20 mM sodium phosphate buffer was added in the mixture. The final mixture was incubated for 4 min at room temperature. After the incubation, 20 μ in the final mixture was transferred into a borosilicated test tube. Then, relative CL intensity for each sample was measured with the luminometer based on the procedure described above.

2.4. Effect of phenol derivatives in ODI-CL reaction

In order to study the effect of phenol derivatives in ODI-CL reaction, 10 μM resorufin (60 μl) in sodium phosphate buffer (pH 8, 20 mM) was mixed with additional sodium phosphate buffer (60 μl) not containing or containing one of phenol derivatives (1 mM). Relative CL intensity of light emitted in the mixture (20 μl) transferred into a test tube was measured for 2 or 3 s using the luminometer with two syringe pumps. The effect of phenol derivatives in ODI-CL reaction was investigated using the experimental data.

2.5. ODI-CLEIA in the presence of phenol red and BSA

Based on the preliminary experimental results using HRP enzyme assay with ODI-CL detection, highly sensitive ODI-CLEIA in the presence of phenol red and BSA was designed for the quantification of CEA in human serum. 6 different CEA standards (0, 2.5, 10, 25, 50, 100 ng/ml) in diluent solution, purchased from Monobind, and patient human serum samples were prepared. Each standard or a patient sample (25 μl) and CEA detection antibody-conjugated HRP (100 μl) were mixed with CEA capture antibody coated on the surface of strip-well. The mixture was stirred for 30 s and incubated for 30 min at room temperature. After the incubation, each strip-well was washed 5 times with phosphate buffered saline containing 0.5% Tween 20 (PBST). After the washing procedure, 20 mM sodium phosphate buffer (pH 8, 100 μl) containing 1 μM Amplex Red, 1 mM phenol red, 1.5 mM H_2O_2 and BSA (1.5 mg/ml) was added in the strip-well. The mixture in the strip-well was incubated for 8 min at room temperature. After the incubation, 20 μl in the strip-well was transferred into a borosilicated test tube. Relative CL intensity of light in a test tube was measured with the luminometer through the same procedure described above. A calibration curve was obtained using relative CL intensities measured from the six standards. Then, the concentration of CEA in unknown sample was determined with the calibration curve.

3. Results and discussion

3.1. Effect of phenol derivatives in ODI-CL enzyme assay in Tris–HCl

Tris–HCl (pH 8) is widely applied as a buffer solution for the enzyme reaction between Amplex Red and H_2O_2 in the presence of HRP. Based on the previous reports (Choi et al., 2010; Chong et al., 2013; Choi et al., 2017), we first studied the effect of 4 different phenol derivatives (PD) in the enzyme assay with ODI-CL detection.

As shown in Fig. 1(A), the relative CL_0 intensity was enhanced with the extension of incubation time for the enzyme reaction in the absence of PD.

Fig. 1(B) shows that the relative CL_{PR} intensity measured after the 10-min enzyme reaction in the presence of phenol red (PR) was the highest. Additionally, the light emitted from the enzyme reaction in the presence of PD was brighter than that emitted from the enzyme immunoassay in the absence of PD. This result indicates that PR acts as an enhancer in the enzyme reaction.

Fig. 1(C) shows that the relative CL_{CPR} was dependent on the

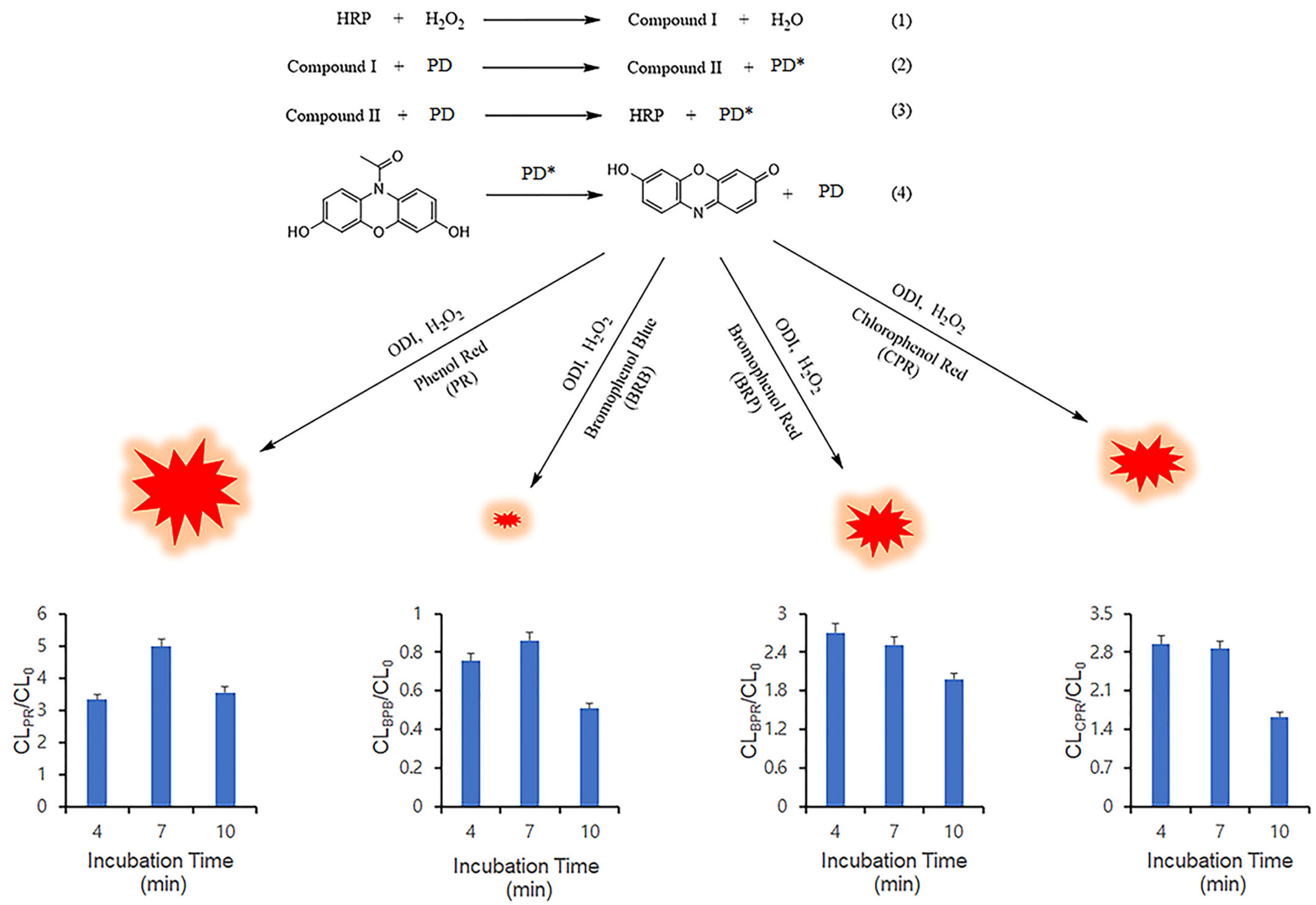

Fig. 2. Possible mechanism of enzyme and ODI-CL reactions in the presence of PD.

enzyme reaction time in the presence of chlorophenol red (CPR). The relative CL_{CPR} intensity was also higher than the relative CL_0 intensity because CPR is an enhancer in the enzyme reaction. However, the brightness of light measured after the 10-min enzyme reaction was slightly higher than that the 7-min enzyme reaction. This result indicates that the enzyme reaction in the presence of CPR is faster than that in the absence of PD.

Fig. 1(D) shows that the relative CL_{BPB} intensity was enhanced with the extension of the enzyme reaction time. Also, Fig. 1(D) indicates that the enzyme reaction with CPR was faster than that with no PD because the relative CL_{BPB} after the 10-min enzyme reaction was slightly higher than that after the 7-min enzyme reaction. However, the results of Fig. 1(D) indicate that BRB is not acting as an enhancer in the enzyme reaction because the relative CL_{BRB} intensity is lower than the relative CL_0 intensity. In general, various types of chlorophenol, such as 2,4,6-trichlorophenol, pentachlorophenol, act as a quencher in ODI-CL reaction. Based on the previous reports, it is possible that BRB also acts as a quencher in ODI-CL reaction.

Fig. 1(E) shows that the relative CL_{BPR} intensity was dependent on the enzyme reaction time. The trend of enzyme reaction in the presence of bromophenol red (BPR) is similar to that in the presence of PR. Thus, BPR can be applied as an enhancer in the enzyme reaction. However, the relative CL_{BPR} intensity was lower than the relative CL_{PR}.

Based on the results of Fig. 1(A~E), we confirmed that resorufin is formed from the enzyme reaction between Amplex Red and H_2O_2 in the presence of HRP with or without an enhancer. As shown in Scheme 1, resorufin emits red light with the addition of ODI-CL reagents. Fig. 1(F) shows that PR, CPR, BPB, and BPR are quenchers in ODI-CL reaction. In particular, BPR is the strongest quencher capable of reducing the brightness of resorufin emitted in ODI-CL reaction. Based on the result, we were able to confirm the reason why the relative CL_{BPB} intensity was lower than relative CL_0 intensity, as shown in Fig. 1(A–D), even though the concentration of resorufin formed from the enzyme reaction in the presence of BPB was higher than that in the absence of PD.

The results shown in Fig. 1 indicate that ODI-CLEIA in the presence of PD, except for BPB, is more sensitive than that in the absence of PD.

3.2. Possible mechanism of enzyme reaction of Amplex red and H_2O_2 in the presence of HRP and PD with ODI-CL detection

As shown in Fig. 2, the possible mechanism of HRP enzyme reaction in the presence of PD is similar to that in the presence of *p*-iodophenol (Kim et al., 2014). The reaction (1) in Fig. 2 shows that HRP converts to compound I in the presence of H_2O_2. Compound II and PD* are formed from the oxidation reaction between compound I and PD as shown in the reaction (2). Also, the reaction (3) indicates that PD* and HRP are formed from the reaction of compound II and the rest of PD. Then, resorufin is formed from the interaction between Amplex Red and PD* as shown in the reaction (4). Finally, resorufin emits light with the addition of ODI-CL reagents such as H_2O_2 and ODI (Lee et al., 2010). Relative CL_{PD} intensity was determined by PD used in HRP enzyme reaction. CL_{PD} is the relative CL intensity in the presence of PD. As shown in Fig. 1, the relative CL_{PR} intensity was the highest. Thus, the ratio of CL_{PR} to CLo (CL_{PR}/CL_0) is the largest. CL_{PR} is the relative CL intensity in the presence of PR. CL_0 is the relative CL intensity in the absence of PD such as PR, BPB, BPR, and CPR. Fig. 2 indicates that the appropriate incubation time for the HRP enzyme reaction in the presence of PR was 7 min.

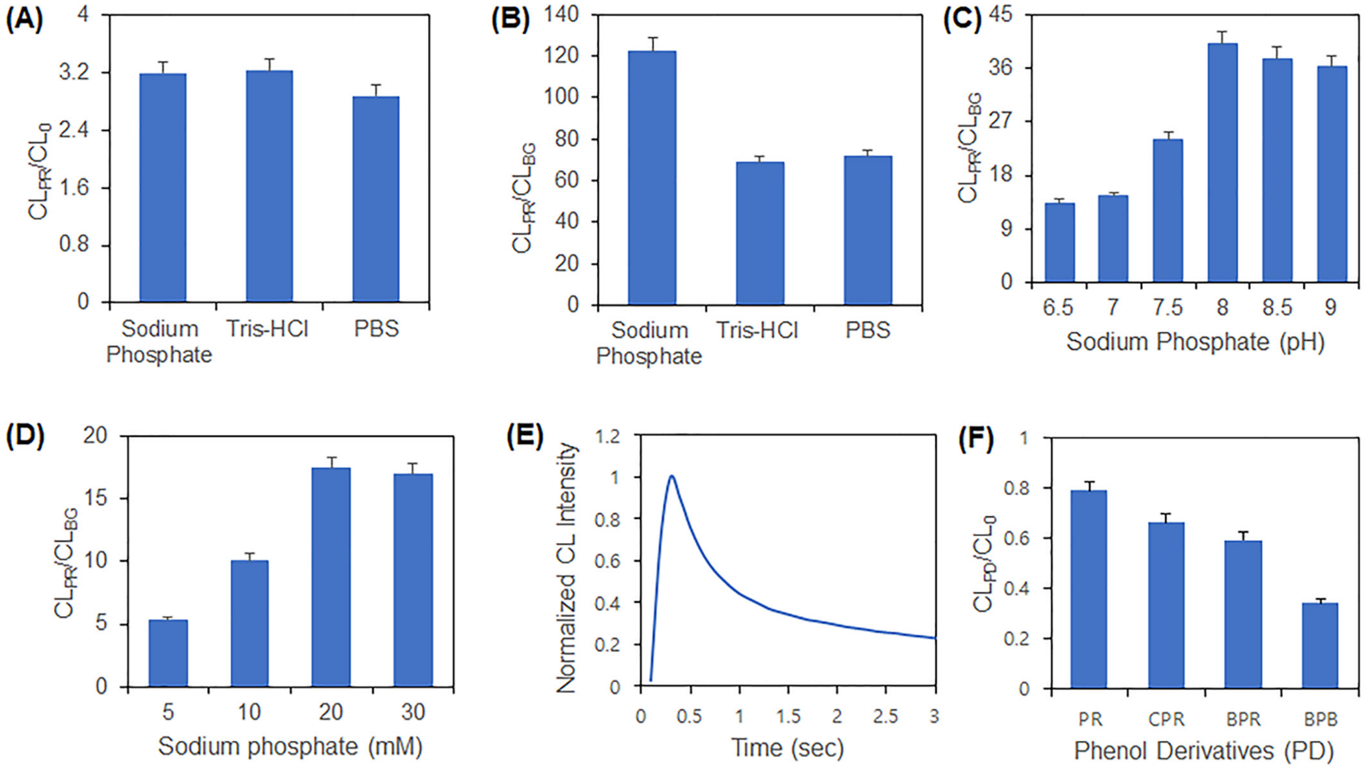

Fig. 3. (A) CL_{PR}/CL_0 of resorufin formed from enzyme reaction operated in 3 different buffers. CL_0 and CL_{PR} were measured in the absence and presence of phenol red (1 mM), (B) CL_{PR}/CL_{BG} of resorufin formed from enzyme reaction operated in 3 different buffers. CL_{BG} was measured in the absence of HRP (0.5 mU/ml), (C) CL_{PR}/CL_{BG} of resorufin formed from enzyme reaction operated in different pH of sodium phosphate buffer (10 mM), (D) CL_{PR}/CL_{BG} of resorufin formed from enzyme reaction operated in different concentration of sodium phosphate buffer (pH 8), (E) CL spectrum of resorufin in the absence of PD, (F) CL_{PD}/CL_0 of resorufin (10 µM) emitted in ODI-CL reaction. (For interpretation of the references to colour in this figure legend, the reader is referred to the web version of this article.)

3.3. Determination of buffer for the HRP enzyme reaction in the presence of PR

Fig. 3(A) shows that the CL_{PR}/CL_0 in HRP enzyme reactions in sodium phosphate buffer (pH 8) is the same as that in Tris–HCl (pH 8) which is the conventional buffer for HRP enzyme assay using Amplex Red and H_2O_2. Also, CL_{PR}/CL_{BG} in sodium phosphate buffer was about two-fold larger than that in Tris–HCl buffer as shown in Fig. 3(B). CL_{BG} is the background measured in the absence of HRP. The results indicate that sodium phosphate buffer is better than Tris–HCl buffer for the HRP enzyme reaction in the presence of PR. Based on the results shown in Fig. 3(C and D), we confirmed that the HRP enzyme reaction in the presence of PR is 20 mM sodium phosphate buffer (pH 8).

Fig. 3(E) shows the CL emission spectrum of resorufin without PD in sodium phosphate buffer (pH 8). The time ($\boldsymbol{\tau}_{\mathbf{max}}$) necessary for attaining the maximum CL intensity ($\mathbf{I}_{\mathbf{max}}$) was as fast as 0.3 s. Also, the time ($\boldsymbol{\tau}_{\mathbf{1/e}}$) necessary for dropping down $CL_{1/e}$ from $\mathbf{I}_{\mathbf{max}}$ was 1.6 s. Fig. 3(F) shows that PR, CPR, BPR, and BPB in sodium phosphate buffer are acting as quenchers in ODI-CL reaction. However, τmax and τ1/e in the presence of PD were the same as those in the absence of PD within statistically acceptable error range (5%).

3.4. Effects of reagents for HRP enzyme reaction

Fig. 4(A) shows that $\tau_{1/e}$ (1.2 s) in sodium phosphate is shorter than that (2 s) in Tris–HCl even though $\boldsymbol{\tau}_{\mathbf{max}}$ (0.3 s) in sodium phosphate is the same as that in Tris–HCl. The results indicate that the life-time of CL emission is dependent on the components existing in a buffer.

Fig. 4(B) shows that the best concentration of PR for the HRP enzyme reaction is 1 mM. The relative CL_{PR} in the presence of 1 mM PR was higher than those in the presence of the rest of the PR concentrations. Based on the results, we selected 1 mM PR for the development of ODI-CLEIA for the quantification of CEA in human serum.

As shown in Fig. 4(C), the relative CL_{PR} intensity in the presence of 1.5 mM H_2O_2 was slightly higher than those in the presence of the rest H_2O_2 concentrations. Based on the results, we selected 1.5 mM H_2O_2 for further research.

Fig. 4(D) shows that the relative CL_{PR} intensity was enhanced with the increase of Amplex Red. We obtained the non-linear curve in this condition because the relative CL_{PR} intensities of resorufin in the presence of 4 and 8 mM Amplex Red were slightly self-quenched. Thus, 2 µM Amplex Red was selected in this research.

Fig. 4(E) shows that the best incubation time range for the HRP enzyme reaction in the presence of BSA and PR is from 8 to 9 min. Based on the research results, we selected the 8-min incubation to develop a highly sensitive ODI-CLEIA capable of rapidly quantifying CEA in human serum.

As shown in Fig. 4(F), the relative CL_{PR} intensity in the HRP enzyme reaction with ODI-CL detection was dependent on the concentration of BSA. The relative CL_{PR} intensity in the presence of 1.5 mg/ml BSA was 12-fold higher than that in the absence of BSA. This is because BSA, as a stabilizer of HRP, can support the activation of HRP in the HRP enzyme reaction shown in Fig. 2 (Dotsikas and Loukas, 2004). In conclusion, the relative $CL_{BSA\text{-}PR}$ intensity was about 70-fold higher than the relative CL_0 measured from the HRP enzyme reaction in the absence of BSA and PR.

In order to study in detail the effect of BSA in ODI-CL enzyme assay, we conducted experiments under the three different reaction conditions shown in Fig. 4(G~I). Fig. 4(G) shows that the relative CL intensity of resorufin was constant in the presence of different concentrations of BSA. The results indicate that BSA is not working as an enhancer in ODI-CL reaction. However, Fig. 4(H) shows that BSA acts as a quencher

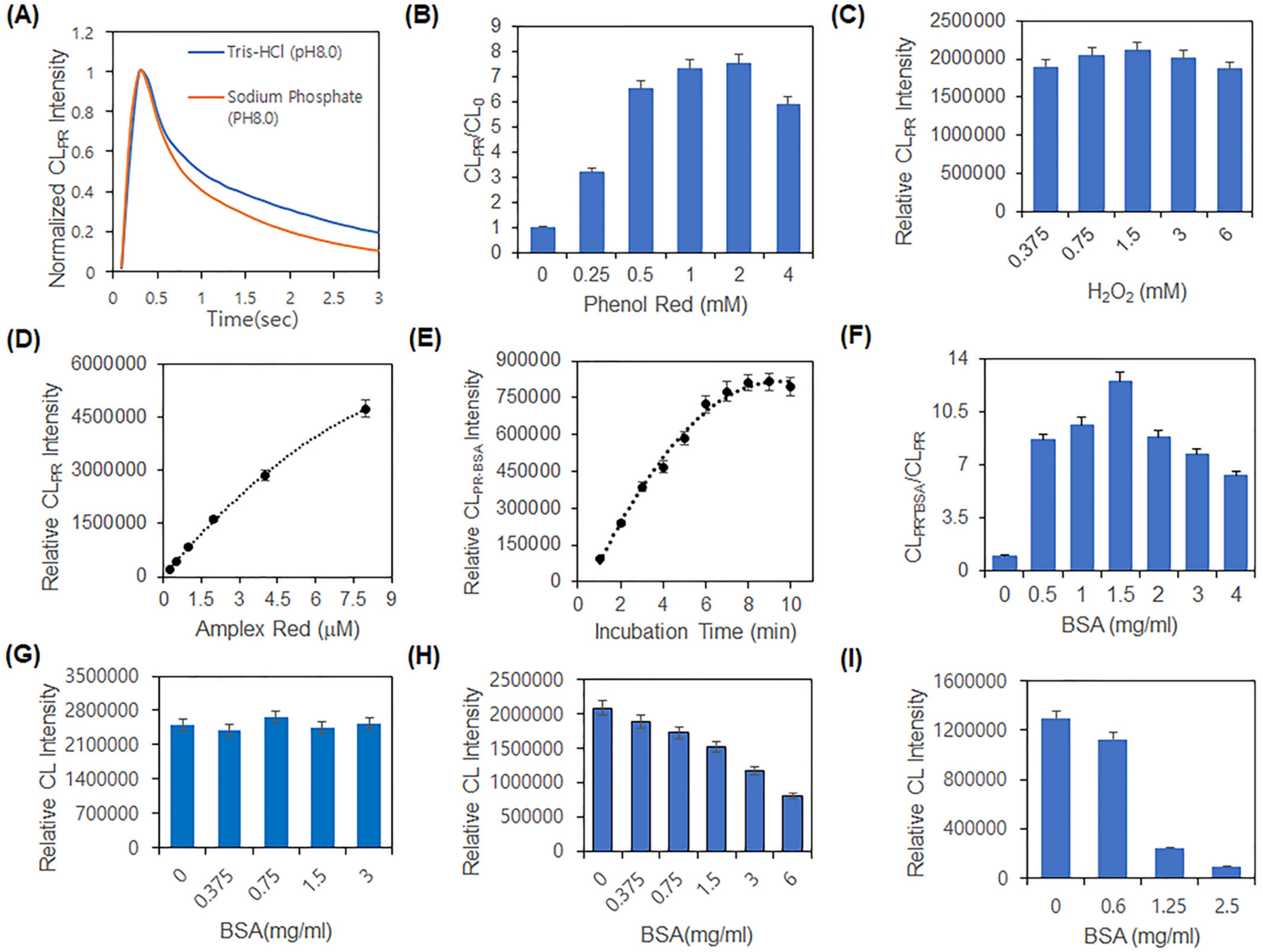

Fig. 4. (A) CL spectra of resorufin in sodium phosphate (pH 8) and Tris–HCl (pH 8), (B) CL_{PR}/CL_0 of resorufin formed from enzyme reaction operated in the presence of different concentrations of phenol red. CL_0 and CL_{PR} were measured in the absence and presence of phenol red, (C) Effect of H_2O_2 in ODI-CL enzyme assay in the presence of Amplex Red (2 µM), HRP (2 mU/ml) and phenol red (1 mM), (D) Effect of Amplex Red in ODI-CL enzyme assay in the presence of H_2O_2 (1.5 mM), HRP (2 mU/ml), and phenol red (1 mM), (E) Determination of incubation time for the analysis of HRP using ODI-CL enzyme assay in the presence of Amplex Red (2 µM), BSA (1.5 mg/ml), H_2O_2 (1.5 mM), HRP (2 mU/ml), and phenol red (1 mM) in sodium phosphate buffer (pH 8), (F) Effect of BSA in ODI-CL enzyme assay in the presence of Amplex Red (2 µM), H_2O_2 (1.5 mM), HRP (2 mU/ml), and phenol red (1 mM) in sodium phosphate buffer (pH 8), (G) Effect of BSA in ODI-CL reaction in the presence of resorufin (1 µM) in sodium phosphate buffer (pH 8), (H) Effect of BSA in ODI-CL enzyme assay in the absence of phenol Red in sodium phosphate buffer (pH 8), reagents: Amplex Red (2 µM), H_2O_2 (1.5 mM), HRP (2 mU/ml), (I) Effect of BSA in ODI-CL enzyme assay in Tris–HCl (pH 8), reagents: Amplex Red (2 µM), H_2O_2 (1.5 mM), HRP (2 mU/ml), and phenol red (1 mM). (For interpretation of the references to colour in this figure legend, the reader is referred to the web version of this article.)

in ODI-CL enzyme assay because the relative CL intensity of resorufin, formed from the enzyme reaction in the absence of PR, was proportionally decreased with the increase of BSA. Additionally, Fig. 4(I) shows that BSA in ODI-CL enzyme assay in the presence of PR acts as a quencher in Tris–HCl (pH 8). However, BSA in ODI-CL enzyme assay in the presence of PR acts as an enhancer in sodium phosphate buffer (pH 8) as shown in Fig. 4(F). These results indicate that the role of BSA is determined by the property of the buffer used in in ODI-CL enzyme assay in the presence of PR.

In conclusion, based on the results shown in Fig. 4(F~I), BSA acts as an enhancer with the combination of BSA and PR in ODI-CL enzyme assay in sodium phosphate buffer (pH 8). However, it acts as a quencher in ODI-CL enzyme assay in the absence of PR or in Tris–HCl (pH 8) containing PR.

3.5. ODI-CLEIA in the presence of PR and BSA

Fig. 5 shows the procedure of ODI-CLEIAs operated under the three different HRP enzyme reaction pathways. CEA and CEA detection antibody-conjugated HRP were added into a strip-well containing CEA capture antibody. The mixture was incubated for 30 min at room temperature. After the incubation, CEA detection antibodies remaining in the strip-well were removed with the washing process. Then, one of mixtures (see components of 1,2,3 shown in Fig. 5) was put in the strip-well for the HRP enzyme reaction for 8 min at room temperature. Finally, each strip-well emitted red light when H_2O_2 and ODI were added.

Fig. 6(A) shows the ODI-CLEIA in the presence of PR and BSA is more sensitive than that in the presence of PR only. The dynamic range of the both ODI-CLEIAs capable of sensing CEA in human serum was from 2.5 to 100 ng/ml. The limits of detection (LOD = 3σ/slope) determined in ODI-CLEIAs in the absence and presence of BSA were as low as 0 46 and 0.19 ng/ml. σ is the standard deviation of background

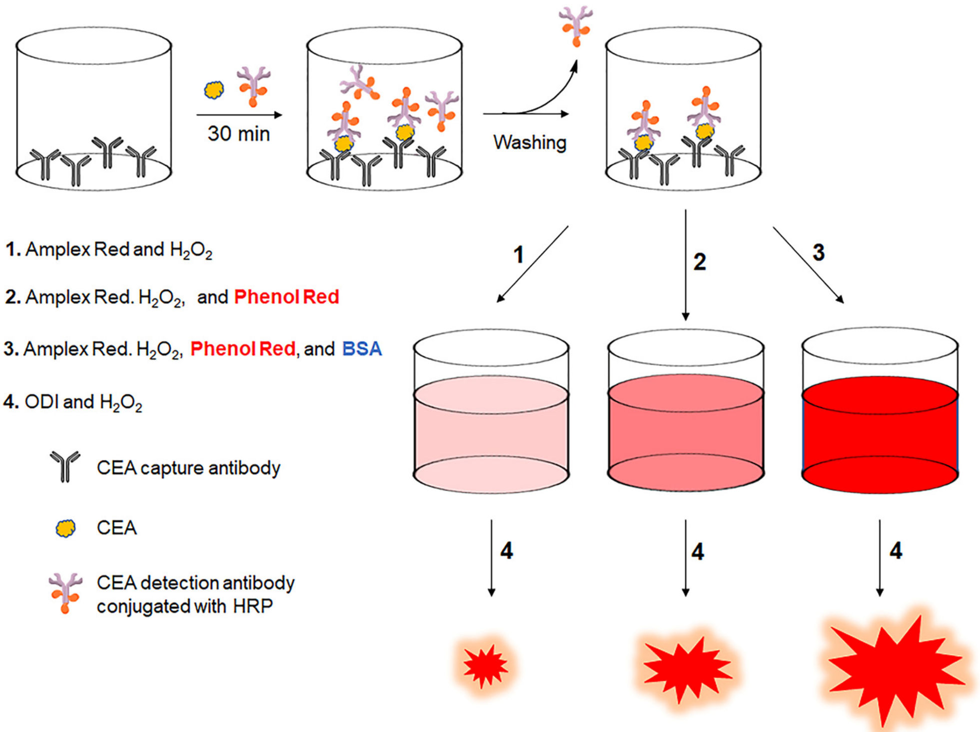

Fig. 5. Procedure of ODI-CLEIAs in the absence and presence of phenol red and BSA. Amplex Red and H_2O_2 are substrates of ODI CLEIA. Phenol Red is an enhancer and BSA is a stabilizer in ODI CLEIA. (For interpretation of the references to colour in this figure legend, the reader is referred to the web version of this article.)

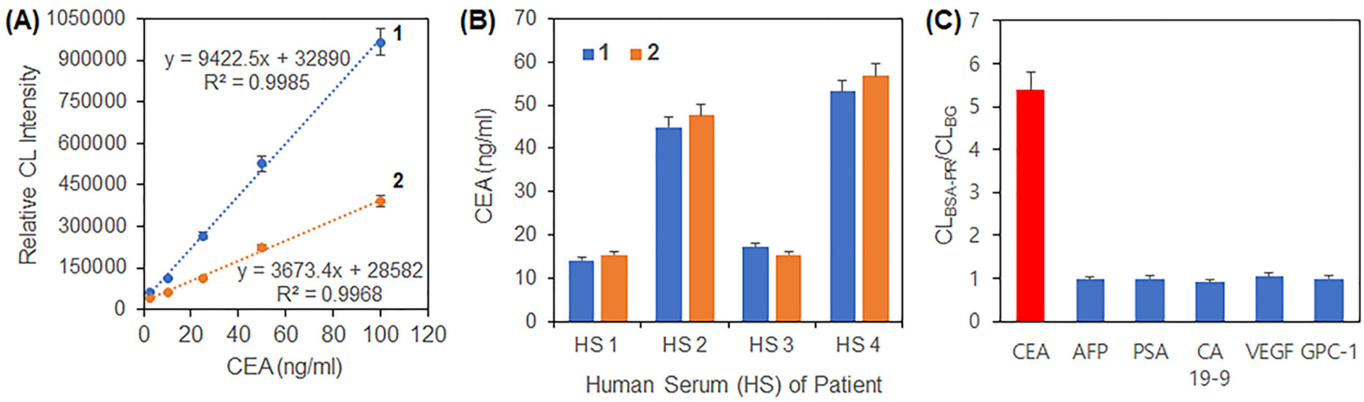

Fig. 6. (A) Calibration curves generated from ODI-CL enzyme immunoassay for the quantification of CEA in human serum. **1**. ODI-CL enzyme immunoassay in the presence of BSA (1.5 mg/ml) and phenol red (1 mM), **2**. ODI-CL enzyme immunoassay in the presence of phenol red only. (B) Correlation of ODI-CL enzyme immunoassay operated under two different conditions. **1**. ODI-CL enzyme immunoassay in the presence of BSA (1.5 mg/ml) and PR (1 mM), **2**. ODI-CL enzyme immunoassay in the presence of PR only. (C) Selectivity of ODI-CL enzyme immunoassay in the presence of BSA and phenol red. Concentration of tumor markers: [CEA] = 10 ng/ml, [AFP] = 1 μg/ml, [PSA] = 1 μg/ml, [CA 19–9] = 1 KU/ml, [VEGF] = 100 ng/ml, [GPC-1] = 100 ng/ml. (For interpretation of the references to colour in this figure legend, the reader is referred to the web version of this article.)

Table 1
Comparison of methods capable of sensing CEA.

Method	Dynamic range (ng/ml)	Analytical time (min)	LOD (ng/ml)	References
Impedimetric immunobiosensor	0–200	80	1	Yeh et al. (2016)
Dual-aptasensor with CL detection	0–200	36	1	Khang et al. (2017)
Dual-label time-resolved fluoroimmunoassay	5–500	50	0.85	Lin et al. (2014)
Time-resolved fluorescence immunoassay	1–1000	65	0.5	Hou et al. (2012)
SWCNTs@GQDs composites as nanocarriers for enzyme-free dual-signal amplification electrochemical immunoassay	0.05–0.65	50	0.005	Luo et al. (2018)
Potential-resolved electrochemiluminescence immunoassay	0.000025–0.02	80	0.00001	Babamiri et al. (2017)
ODI-CLEIA in the presence of PR and BSA	2.5–100	38	0.19	This research
ODI-CLEIA in the presence of PR only	2.5–100	38	0.46	This research

Table 2
Accuracy, precision, and recovery of ODI-CLEIA in the presence of BSA and PR. $N = 5$.

Sample	Spiked (ng/ml)	Detected (ng/ml)	Recovery (%)
1	5	4.74 (± 0.2)	94.8
2	10	11.05 (± 0.45)	110.5
3	25	27.29 (± 1.58)	109.2
4	50	48.77 (± 3.85)	97.5

Table 3
Intra-assay and inter-assay of ODI-CLEIA in the presence of BSA and PR for the analysis of CEA in human serum.

Intra-assay				Inter-assay			
N[a]	Average (ng/ml)	SD[b]	C.V. (%)	N[a]	Average (ng/ml)	SD[b]	C.V. (%)
5	3.75	0.22	5.86	21	3.88	0.36	9.27
5	15.72	0.84	5.34	21	15.62	0.91	5.82
5	34.54	2.25	7.23	21	35.94	2.71	7.54

[a] Number of samples.
[b] Standard deviation.

consecutively measured 20 times. As shown in Table 1, LOD of the ODI-CLEIAs was as low as those of other enzyme immunoassays recently reported (Hou et al., 2012; Lin et al., 2014; Yeh et al., 2016; Khang et al., 2017). LODs of analytical methods reported by two research groups (Babamiri et al., 2017; Luo et al., 2018) shown in Table 1 were much lower than those of ODI-CLEIAs and other methods (Hou et al., 2012; Lin et al., 2014; Yeh et al., 2016; Khang et al., 2017). This is because the cut-off value (5 ng/ml) of CEA in human serum is beyond the dynamic ranges of these two methods. In other words, ODI-CLEIAs and other methods (Hou et al., 2012; Lin et al., 2014; Yeh et al., 2016; Khang et al., 2017) are appropriate for the quantification of CEA in 100% human serum because the cut-off value of CEA is in the dynamic ranges determined using those methods.

Fig. 6(B) shows the good correlation between ODI-CLEIA in the presence of BSA and PR and ODI-CLEIA in the presence of PR only. Also, Fig. 6(C) shows ODI-CLEIA developed in this research can quantify CEA in human serum with the excellent selectivity.

As shown Table 2, the range of recovery for the ODI-CLEIA in the presence of BSA and PR was from 94.8% to 110.5%. Additionally, Table 2 shows that accuracy and precision of the ODI-CLEIA were good within the statistically acceptable error range.

We studied the intra- and inter-assay for the ODI-CLEIA in the presence of BSA and PR as shown in Table 3. The confidence variable (CV) range of the intra-assay was 5.34–7.23%. Also, the inter-assay was performed for 7 consecutive days with the same samples used in the intra-assay. The CV range of the intra-assay was 5.74–7.05%. These results indicate that the ODI-CLEIA in the presence of BSA and PR can be applied as a new analytical method to quantify CEA in human serum with acceptable precision.

4. Conclusions

We confirmed that phenol derivatives (PD) such as PR, BPR, and CPR can be applied as an enhancer in HRP enzyme assay with ODI-CL detection. Also, we were able to enhance the sensitivity of HRP enzyme assay with the addition of BSA capable of supporting the activation of HRP. Using the advantages of PR and BSA in HRP enzyme assay, the CL emission formed in HRP enzyme reaction in the presence of PR and BSA was about 70-fold brighter than that in the absence of PR and BSA.

Based on the preliminary research results, ODI-CLEIA in the presence of PR and BSA was developed to rapidly quantify trace levels of CEA in human serum. Based on the statistically good results (e.g., accuracy, precision, recovery, selectivity) for the ODI-CLEIA in the presence of BSA and PR, in conclusion, we expect that the new analytical method can be applied in various fields such as biochemistry, clinical chemistry, environmental science, public health, and toxicology.

Conflicts of interest

There are no conflicts of interest to declare.

Acknowledgement

This project was performed based on the research program (LMD-0915) of Luminescent MD, LLC.

References

Ahn, J., Shin, Y.B., Lee, J., Kim, M.G., 2015. Human alpha-fetal protein immunoassay using fluorescence suppression with fluorescent-bead/antibody conjugate and enzymatic reaction. Biosens. Bioelectron. 71, 115–120.

Babamiri, B., Hallaj, R., Salimi, A., Akhtari, K., 2017. Potential-resolved electrochemiluminescence immunoassay for simultaneous determination of CEA and AFP tumor markers using dendritic nanoclusters and Fe3O4@SiO2 nanoparticles. Microchim. Acta 184, 3613–3623.

Barni, F., Lewis, S.W., Berti, A., Miskelly, G.M., Lago, G., 2007. Forensic application of the luminol reaction as a presumptive test for latent blood detection. Talanta 72, 896–913.

Bodulev, O.L., Gribas, A.V., Sakharov, I.Y., 2018. Microplate chemiluminescent assay for HBV DNA detection using 3-(10 '-phenothiazinyl)propionic acid/N-morpholinopyridine pair as enhancer of HRP-catalyzed chemiluminescence. Anal. Biochem. 543, 33–36.

Chen, G., Jin, M.J., Du, P.F., Zhang, C., Cui, X.Y., Zhang, Y., Wang, J., Jin, F., She, Y.X., Shao, H., Wang, S.S., Zheng, L.F., 2017. A review of enhancers for chemiluminescence enzyme immunoassay. Food Agric. Immunol. 28, 315–327.

Choi, J., Kim, Y.T., Lee, J.H., 2010. Rapid quantification of melamine in milk using competitive 1,1 '-oxalyldiimidazole chemiluminescent enzyme immunoassay. Analyst 135, 2445–2450.

Choi, G., Kim, E., Park, E., Lee, J.H., 2017. A cost-effective chemiluminescent biosensor capable of early diagnosing cancer using a combination of magnetic beads and platinum nanoparticles. Talanta 162, 38–45.

Chong, R., Rho, J.E.R., Yoon, H.J., Park, P.S., Rho, T.H.D., Park, J.Y., Park, L., Kim, Y.H., Lee, J.H., 2013. Role of triton X-100 in chemiluminescent enzyme immunoassays capable of diagnosing genetic disorders. Talanta 116, 403–408.

Dotsikas, Y., Loukas, Y.L., 2004. Employment of 4-(1-imidazolyl)phenol as a luminol signal enhancer in a competitive-type chemiluminescence immunoassay and its comparison with the conventional antigen-horseradish peroxidase conjugate-based assay. Anal. Chim. Acta 509, 103–109.

Engvall, E., Perlmann, P., 1971. Enzyme-linked immunosorbent assay (ELISA) quantitative assay of immunoglobulin-g. Immunochemistry 8, 871.

Feng, X.L., Ren, H.L., Li, Y.S., Hu, P., Zhou, Y., Liu, Z.S., Yan, D.M., Hui, Q., Liu, D., Lin, C., Liu, N.N., Liu, Y.Y., Lu, S.Y., 2014. A magnetic particles-based chemiluminescence enzyme immunoassay for rapid detection of ovalbumin. Anal. Biochem. 459, 12–17.

Hou, J.Y., Liu, T.C., Lin, G.F., Li, Z.X., Zou, L.P., Li, M., Wu, Y.S., 2012. Development of an immunomagnetic bead-based time-resolved fluorescence immunoassay for rapid determination of levels of carcinoembryonic antigen in human serum. Anal. Chim. Acta 734, 93–98.

Khang, H., Cho, K., Chong, S., Lee, J.H., 2017. All-in-one dual-aptasensor capable of rapidly quantifying carcinoembryonic antigen. Biosens. Bioelectron. 90, 46–52.

Kim, J., Kim, J., Rho, T.H.D., Lee, J.H., 2014. Rapid chemiluminescent sandwich enzyme immunoassay capable of consecutively quantifying multiple tumor markers in a sample. Talanta 129, 106–112.

Lee, J.H., Rock, J.C., Park, S.B., Schlautman, M.A., Carraway, E.R., 2002. Study of the characteristics of three high-energy intermediates generated in peroxyoxalate chemiluminescence (PO-CL) reactions. J. Chem. Soc.-Perkin Trans. 2, 802–809.

Lee, J.H., Rho, J.E.R., Rho, T.H.D., Newby, J.G., 2010. Advent of innovative chemiluminescent enzyme immunoassay. Biosens. Bioelectron. 26, 377–382.

Lee, Y., Kim, S.S., Lee, J.H., 2019. Chemiluminescent dual-enzyme immunoassays capable of simultaneously quantifying carbohydrate antigen 19–9 and carcinoma embryonic antigen in a sample. Anal. Chim. Acta 1060, 88–96.

Lin, G.F., Zhao, H., Liu, T.C., Hou, J.Y., Ren, Z.Q., Huang, W.H., Dong, W.Q., Wu, Y.S., 2014. Simultaneous determination of the cytokeratin 19 fragment and carcinoembryonic antigen in human serum by magnetic nanoparticle-based dual-label time-resolved fluoroimmunoassay. RSC Adv. 4, 55229–55236.

Liu, M.Y., Jia, C.P., Jin, Q.H., Lou, X.H., Yao, S.H., Xiang, J.Q., Zhao, J.L., 2010. Novel colorimetric enzyme immunoassay for the detection of carcinoembryonic antigen. Talanta 81, 1625–1629.

Liu, J., Zhang, L.L., Fu, C.Y., Wang, Y.S., Sun, S.H., 2015. Employment of 4-(1,2,4-triazol-1-yl)phenol as a signal enhancer of the chemiluminescent luminol-H_2O_2-horseradish peroxidase reaction for detection of hepatitis C virus in real samples. Luminescence 30, 1297–1302.

Liu, Z.J., Wei, X., Xu, H., Li, M., Zhu, G.B., Xue, Y.L., Zhang, Z., Zhao, G.D., Du, D.L., 2016. Sensitive detection of thiacloprid in environmental and food samples by enhanced chemiluminescent enzyme immunoassay. RSC Adv. 6, 29460–29465.

Luo, Y.N., Wang, Y.X., Yan, H.Y., Wu, Y., Zhu, C.Z., Du, D., Lin, Y.H., 2018. SWCNTs@GQDs composites as nanocarriers for enzyme-free dual-signal amplification electrochemical immunoassay of cancer biomarker. Anal. Chim. Acta 1042, 44–51.

Park, P.S., Rho, T.H.D., Kim, Y.T., Ko, S.O., Schlautman, M.A., Carraway, E.R., Lee, J.H., 2011. Evidence of multiple pathways capable of emitting peroxyoxalate chemiluminescence using a charge coupled device spectrometer. Chem. Commun. 47, 5542–5544.

Park, L., Kim, J., Lee, J.H., 2013. Role of background observed in aptasensor with chemiluminescence detection. Talanta 116, 736–742.

Pei, X.M., Zhang, B., Tang, J., Liu, B.Q., Lai, W.Q., Tang, D.P., 2013. Sandwich-type immunosensors and immunoassays exploiting nanostructure labels: a review. Anal. Chim. Acta 758, 1–18.

Rongen, H.A.H., Hoetelmans, R.M.W., Bult, A., Vanbennekom, W.P., 1994. Chemiluminescence and immunoassays. J. Pharm. Biomed. Anal. 12, 433–462.

Sakamoto, S., Putalun, W., Vimolmangkang, S., Phoolcharoen, W., Shoyama, Y., Tanaka, H., Morimoto, S., 2018. Enzyme-linked immunosorbent assay for the quantitative/qualitative analysis of plant secondary metabolites. J. Nat. Med. 72, 32–42.

Vashist, S.K., van Oordt, T., Schneider, E.M., Zengerle, R., von Stetten, F., Luong, J.H.T., 2015. A smartphone-based colorimetric reader for bioanalytical applications using the screen-based bottom illumination provided by gadgets. Biosens. Bioelectron. 67, 248–255.

Vdovenko, M.M., Zubkov, A.V., Kuznetsova, G.I., Della Ciana, L., Kuzmina, N.S., Sakharov, I.Y., 2010. Development of ultra-sensitive soybean peroxidase-based CL-ELISA for the determination of human thyroglobulin. J. Immunol. Methods 362, 127–130.

Vdovenko, M.M., Demiyanova, A.S., Chemleva, T.A., Sakharov, I.Y., 2012. Optimization of horseradish peroxidase-catalyzed enhanced chemiluminescence reaction by full factorial design. Talanta 94, 223–226.

Wu, Y.Q., Zeng, L.F., Xiong, Y., Leng, Y.K., Wang, H., Xiong, Y.H., 2018. Fluorescence ELISA based on glucose oxidase-mediated fluorescence quenching of quantum dots for highly sensitive detection of hepatitis B. Talanta 181, 258–264.

Yang, X.Y., Guo, Y.S., Wang, A.G., 2010. Luminol/antibody labeled gold nanoparticles for chemiluminescence immunoassay of carcinoembryonic antigen. Anal. Chim. Acta 666, 91–96.

Yeh, C.H., Su, K.F., Lin, Y.C., 2016. Development of an impedimetric immunobiosensor for measurement of carcinoembryonic antigen. Sens. Actuator A-Phys. 241, 203–211.

Yu, F.Y., Vdovenko, M.M., Wang, J.J., Sakharov, I.Y., 2011. Comparison of enzyme-linked immunosorbent assays with chemiluminescent and colorimetric detection for the determination of ochratoxin A in food. J. Agric. Food Chem. 59, 809–813.

Yu, X.Q., Sheng, Y.Y., Zhao, Y.J., Fan, A.P., 2016. Employment of bromophenol red and bovine serum albumin as luminol signal co-enhancer in chemiluminescent detection of sequence-specific DNA. Talanta 148, 264–271.

Yusakul, G., Udomsin, O., Tanaka, H., Morimoto, S., Juengwatanatrakul, T., Putalun, W., 2015. Enzyme-linked immunosorbent assay by enhanced chemiluminescence detection for the standardization of estrogenic miroestrol in Pueraria candollei Graham ex Benth. Luminescence 30, 568–575.